CHAPTER IV
RESULTS AND DISCUSSION

4.1 Abstract

Generally, the aim of using food packaging is to preserve food products. However, microbial contamination is able to cause food deterioration. Therefore, the antimicrobial substances are often incorporated into packaging materials. In this work, zinc oxide (ZnO) coated polypropylene (PP) film was prepared with the aid of dielectric barrier discharge (DBD) plasma treatment. The surface hydrophilicity of PP film was increased after DBD plasma treatment due to the presence of oxygen-containing functional groups on the plasma-treated PP surface. In addition, the surface roughness of the plasma-treated PP film increased with increasing treatment time. The DBD plasma treatment did not affect the mechanical properties of the PP film. The optimum DBD plasma treatment time was 10 s. The plasma-treated PP film was further immersed in zinc nitrate solution before being converted to zinc oxide particles by reacting with sodium hydroxide. The highest amount of zinc oxide on PP film was 0.26 wt.%. The ZnO-loaded plasma-treated PP film possessed high antibacterial activity against both gram-negative Escherichia coli and gram-positive Staphylococcus auerus.

Keywords: Zinc oxide/ Polypropylene/ Dielectric Barrier Discharge/ Antibacterial activities

4.2 Introduction

One of the most important functions of the food packaging is to preserve food products from sunlight, moisture, temperature, oxygen, and microorganisms. Among a variety of factors capable of affecting the food quality, microorganisms are considered to be the most significant because they can lead to cross contamination, discoloration, stinky adore, and food borne illness. Accordingly, the antimicrobial agents, either organic or inorganic compounds, are always used to minimize the amount of microorganisms in order to maintain the quality of foodstuffs.

In general, there are two approaches to incorporate the antimicrobial agents into food packaging — preparation of composite films and surface coating. However, the resulting composites show low antimicrobial activities because the incorporated antimicrobial agents do not cover the surface of the packaging films. Thus, they are not totally available for antimicrobial activity. On the contrary, the coating is an alternative approach to improve the antimicrobial activity via incorporating the antimicrobial agents into the food contact layer [14].

Zinc oxide (ZnO) is often used as an antimicrobial agent due to its several advantages, such as inexpensive cost, high antimicrobial activities, non-toxicities, high safety, and biocompatibilities. ZnO has been used as a filling in medical materials in diverse fields, including drug delivery, cosmetics, and pharmaceutical [15]. The antimicrobial activities of ZnO are of great interest since it inhibits the microbial growth or kills microorganisms either with or without UV light [8]. Generally, the ZnO particles are frequently tested against Gram-negative and Gram-positive bacteria [18]. Moreover, it can inhibit the growth of fungus, such as *Aspergillus Niger* [17]. Regardless of its antimicrobial activities, ZnO is incorporated into a number of materials for introducing new properties, like photocatalytic activities, electrical conductivities, and resistivity to photo-degradation.

Polypropylene (PP) is commonly used in food packaging because of its many advantages, including abundant supply, inexpensive cost, good resistance to chemical and harsh environment, and excellent moisture barrier. However, the wettability, adhesion, and printability of PP are low [2]. In this study, the dielectric barrier discharge (DBD) plasma technique is chosen to enhance the coating ability of the PP surface. The DBD plasma was used for surface modification by introducing the oxygen-containing functional groups at the surface of materials. Moreover, it also provides many advantages such as environmentally friendly, inexpensive, and easy to operate [7] which make the DBD plasma technique become a favorable technique.

In the present work, ZnO-coated PP films were accomplished with the aid of DBD plasma treatment. The optimum condition for DBD plasma treatment were chosen based on the results of water contact angle measurement, mechanical testing, X-ray photoelectron spectroscopy (XPS), scaning probe microscopy (SPM), and fourier-transformed infrared (FTIR) spectroscopy. The antimicrobial activities of

ZnO-coated plasma-treated PP films at different ZnO contents were also tested against both Gram-negative *Escherichia coli* and Gram-positive *Staphylococcus auerus*.

4.3 Experimental

4.3.1 Chemicals and Materials

4.3.1.1 Materials

PP films were purchased from Somboon Plastic Co., Ltd (Thailand).

4.3.1.2 Chemicals

(a) $Zn(NO_3)_2$, technical grade, was purchased from Ajax Finechem Pty Ltd.

(b) NaOH anhydrous pellets, analytical grade, were purchased from Ajax Finechem Pty Ltd.

4.3.1.3 Air Gas for Plasma Treatment

Air zero (high purity) used in the plasma treatment was obtained from Thai Industrial Gas Co., Ltd. (Thailand).

4.3.2 Equipment

4.3.2.1 Water Contact Angle Measurement

Water contact angle measurement was carried out at room temperature using the sessile drop technique. The contact angle formed between the 10-µl distilled water droplet and the PP surface was measured by a drop shape analysis system (Krüss, DSA10 Mk2). The reported values were the average of five measurements.

4.3.2.2 Lloyd Tensile Tester

Mechanical properties in terms of ultimate tensile strength and elongation at break were measured by using a universal testing machine (Lloyd, LRX). The specimen was cut into a dumb bell shape with the dimension of 6 mm × 1 mm with the gauge area of 6 mm × 1 mm. The load cell, the gauge length, and the displacement rate used during the testing were 2500 N, 5 mm, and 100 mm min^{-1}, respectively. Each reported datum was the mean of ten measurements.

4.3.2.3 ATR-FTIR Spectroscopy

The ATR-FTIR spectroscopy (Thermo Nicolet Nexus, 670) was employed to analyze the surface chemical composition of the PP films both before and after the DBD plasma treatment. All ATR-FTIR spectra were collected using 32 scans in a wavenumber range of 4000 cm^{-1} to 600 cm^{-1} at a resolution of 4 cm^{-1}. All PP specimens subjected to the ATR-FTIR analysis were cut into a precise dimension of 1.0 cm × 7.0 cm.

4.3.2.4 Scanning Electron Microscopy (SEM)

The surface morphology of the synthesized ZnO and the PP specimens were observed under a SEM microscope (Hitachi, S-4800) operated at 2.0 kV. The samples were placed on a brass stub before coated with a thin layer of gold using an ion sputtering device operated at 120 mA for 2 min. The SEM was also operated in the energy dispersive X-ray (EDX) mode in order to qualitatively determine the deposition of zinc oxide (ZnO) on the surface of PP film.

4.3.2.5 Atomic Absorption Spectroscopy (AAS)

An AAS spectrophotometer (Varian spectra, 300/400) was used for the quantitative analysis of the deposition of ZnO on the PP film. The samples were examined by using a hollow cathode lamp with a standard wavelength of 213.9 nm. The concentration of the deposited ZnO was calculated from a calibration curve of Zn^{2+} in the concentration range of 0.4 ppm to 2.0 ppm.

4.3.2.6 Wide Angle X-ray Diffraction (WAXD) Analysis

The crystalline structure of ZnO was characterized by an X-ray diffractometer (Bruker AXS, D8 advance) operated with the use of Cu Kα as the X-ray source. The WAXD analysis was done in a continuous mode with a scan speed of 1° min^{-1} covering the angle (2θ) from 10° to 80°. The WAXD data were also used to calculate the ZnO grain size using the Scherrer formula:

$$D = \frac{\kappa\lambda}{\beta\cos\theta}$$

where D is the grain size, K is 0.89, λ is the X-ray wavelength (0.15 nm), θ is the Bragg diffraction angle, and β is the peak width at half maximum (FWHM).

4.3.2.7 Surface Probe Microscopy (SPM)

The surface topography of the polymeric substrates was investigated by using a scanning probe microscope (SPM) (Veeco, Nanoscope IV) with the tapping mode in air at room temperature. The obtained micrographs were minimally flattened, and high frequency noise was diminished in order to facilitate data analysis.

4.3.2.8 X-ray Photoelectron Spectroscopy (XPS)

The chemical composition of treated PP film and ZnO coated PP films were also analized by Kratos Axis Ultra DLD with the active area 2 mm^2. The XPS spectra were excited by the Al Kα X-ray source (1486.6 eV).

4.3.3 Plasma Treatment and Sample Preparation

The PP-films were cut into a square shape with the dimension of 2 cm× 2 cm before treated with the DBD plasma. The optimum operating conditions for the DBD plasma treatment were selected at the voltage of 50 kV, the frequency of 325 Hz, and the electrode gap of 4 mm under air environment [12]. After that, the treated PP-film was dipped into an aqueous $Zn(NO_3)_2$ solution at different concentrations, followed by a drop wise addition of a 2.5 M NaOH solution. Next, the sample was washed with an excess amount of deionized water and dried in air at the room temperature.

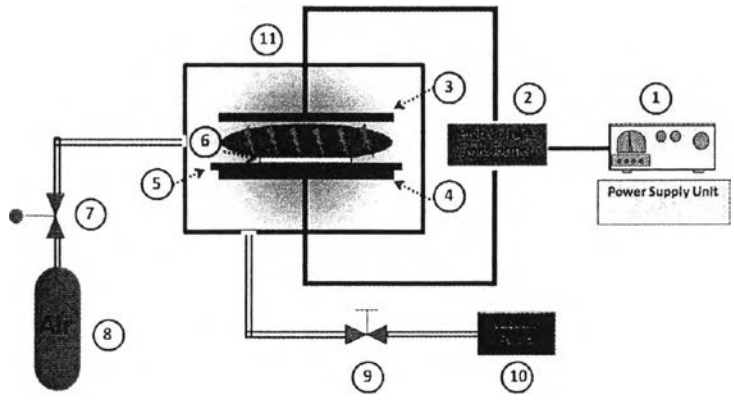

Figure 4.1 The DBD set up (1) power supply unit, (2) high voltage transformer, (3) upper electrode, (4) lower electrode, (5) dielectric glass, (6) Polypropylene film, (7) mass-flow controller, (8) air gas, (9) needle calve, (10) vacuum pump and (11) plasma chamber.

4.3.4 Antibacterial Activity Testing

The E. coli and S. aureus were selected as representatives of Gram-negative and Gram-positive bacteria, respectively. The antimicrobial activities of ZnO nanoparticle-coated DBD plasma-treated PP films were determined based on the two methods.

Antibacterial properties of ZnO-coated PP film were evaluated based on the colony count method using ASTM E 2149-01. First, a culture medium was prepared by mixing 0.3 g of beef extract with 0.5 g of peptone in 100 ml water. The bacterial inoculums were prepared by transferring one colony of each microorganism into 20 ml of a culture medium. After that, the mixture was incubated in a shaking incubator at 150 rpm and 37 °C for 24 h. About 1 ml of the as-prepared inoculums was added into several vials of 9 ml of 0.85% sterile NaCl aqueous solution. Standard serial dilution method was used to obtain an appropriate bacterial concentration, i.e., 10^{-6} for *S. aureus* and 10^{-5} for *E. coli*. Next, the test sample was cut into square shape with the dimension of 2.0 cm × 2.0 cm before added to the

bacterial suspension. The suspension mixture was then incubated in a shaking incubator at 150 rpm and 37 °C. After the contact time interval of 3 h, 100 µl of the suspension was withdrawn and subsequently spread on the sterilized agar plate. Bacterial growth was visualized after an overnight incubation at 37 °C for 24 h [20]. The percentage of bacterial reduction was determined by using the following equation:

$$\text{Bacterial reduction} = \frac{(\text{Viable cell count at 0 h} - \text{Viable cell count at 24 h})}{\text{Viable cell count at 0 h}} \times 100$$

4.4 Results and Discussion

4.4.1 Characterization of DBD Plasma-Treated PP Film

4.4.1.1 Effect of DBD Plasma Treatment Time on Water Contact Angle on PP Film.

The hydrophilic properties of DBD plasma-treated PP film were characterized by water contact angle measurement. Figure 4.2 shows the effect of DBD plasma treatment time on the water contact angle on PP film. Obviously, the water contact angle drastically decreased from 89.7° to 50.4° as the DBD plasma treatment time increased from 0 s to 10 s. A constant water contact angle around 50° at the treatment time longer than 10 s implied a saturation state of surface wettability. The result indicated that the DBD plasma treatment led to an increase in the surface hydrophilicity of PP film. This should be mostly likely due to the presence of new polar functional groups on the plasma-treated surface induced by the active species generated by the air plasma, especially oxygen-based species (NO, NO_2, and N_2O) as well as charged species (NO^+, O_2^+, and O^+), which are very reactive. Thus, a number of new polar functional groups were incorporated into the surface of PP film, resulting in an increment of the hydrophilicity of PP films after plasma treatment [5].

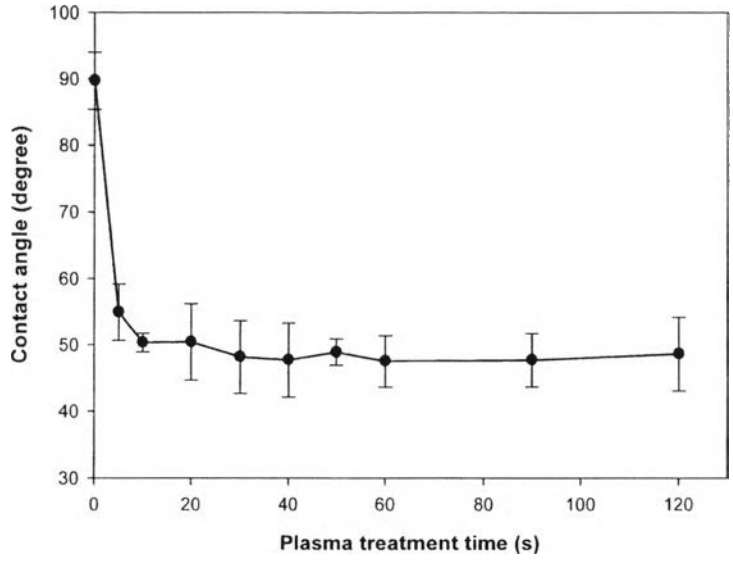

Figure 4.2 Effect of plasma treatment time on water contact angle on PP film.

4.4.1.2 Effect of DBD Plasma Treatment Time on Mechanical Properties of PP Film.

The mechanical properties of DBD plasma treated-PP film were investigated in terms of tensile strength and percentage of elongation at break. As shown in Figures 4.3 (a) and (b), the DBD plasma treatment insignificantly affected both tensile strength and elongation at break of PP film, suggesting that the DBD plasma treatment modified only the top of the PP surface. Therefore, the bulk properties of PP film remained steady after the DBD plasma treatment [19]

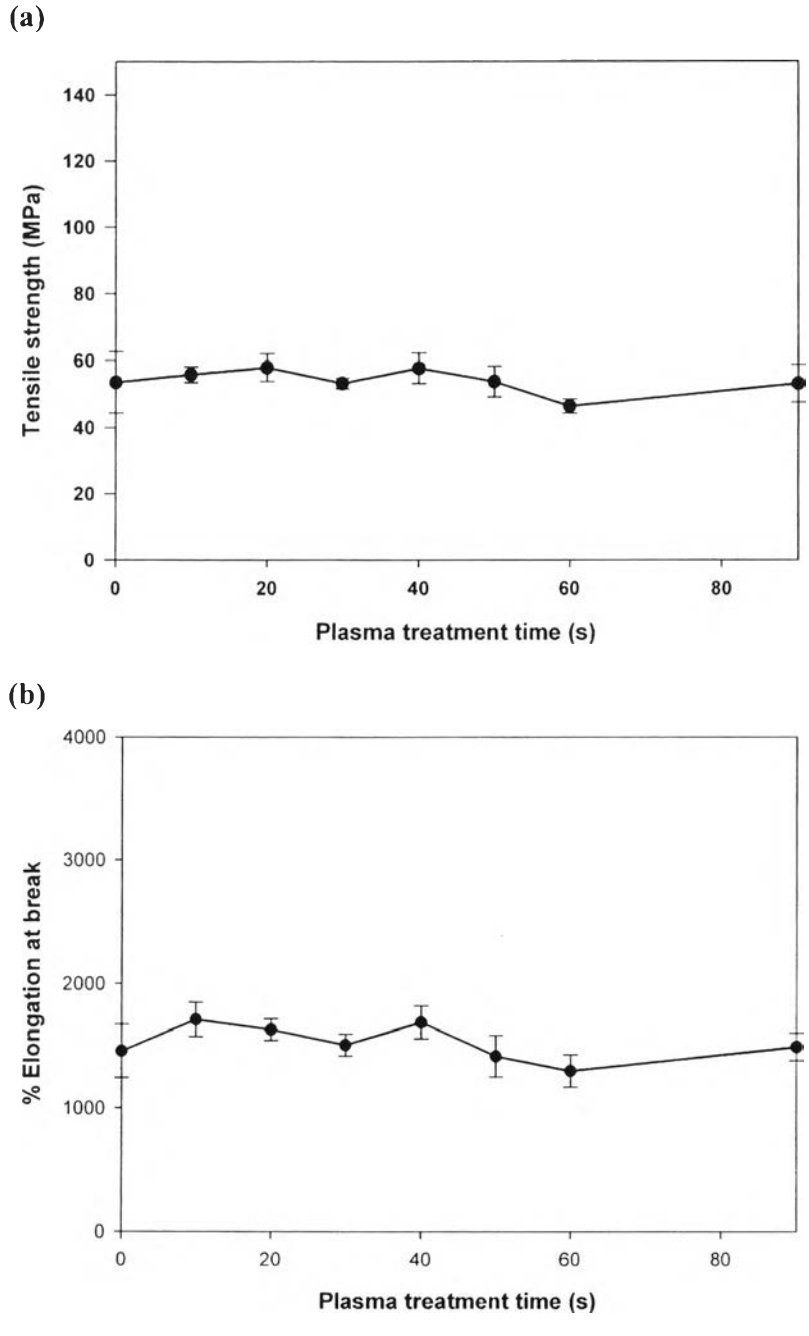

Figure 4.3 Effect of DBD plasma treatment time on (a) tensile strength and (b) elongation at break of PP film.

4.4.1.3 Effect of DBD Plasma Treatment Time on Surface Chemical Composition of PP Film.

The surface chemical composition of DBD plasma-treated PP film was investigated by using the ATR-FTIR technique. Figure 4.4 shows the ATR-FTIR spectra of the PP films before and after the DBD plasma treatment. After the DBD plasma treatment, the new characteristic peaks appeared at the wavenumbers of 1633 cm^{-1}, 1718 cm^{-1}, and 3400 cm^{-1} corresponding to COO^- asymmetrical stretching vibration, C=O stretching vibration, and O-H stretching vibration, respectively [16] . The intensity of new peaks was also found to increase with increasing the DBD plasma treatment time, implying a higher amount of the new oxygen-containing functional groups at a longer treatment time. These new functional groups should relate to an increase in the surface hydrophilicity after the DBD plasma treatment.

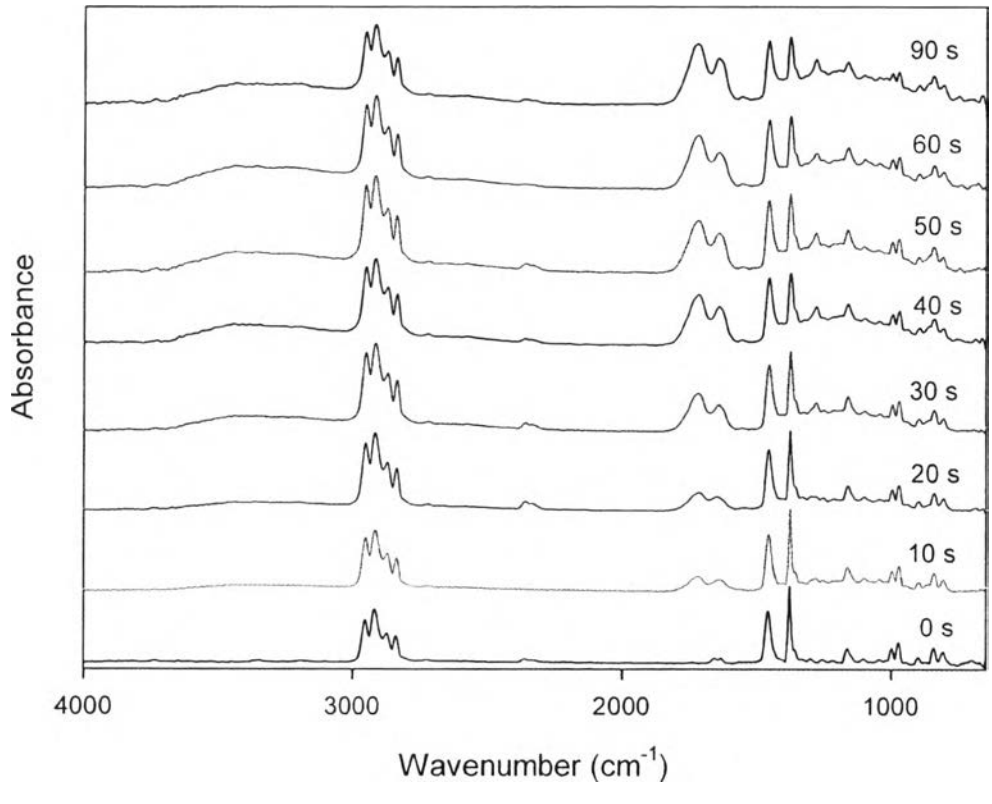

Figure 4.4 ATR-FTIR spectra of PP films at different DBD plasma treatment time.

Moreover, the chemical composition of treated-PP films was further examined using the XPS technique. Figures 4.5 (a) and (b) show the C(1s) spectra of untreated PP films and plasma-treated PP films at 10 s. The result shows that the chemical composition of untreated PP-films is altered after the plasma treatment which can be observed from three main peaks. The peak at 285.0 and 285.8 eV was attributed to C-C/C-H and C-CO_2 bond [5]. The last peak at 287.1 eV was attributed to C-O bond [11]. As shown in table 4.1, the percentage of oxygen-containing polar group which are C-O, C=O and O-C=O are increased as increasing the plasma treatment time whereas the percentage of C-C/C-H was decreased. It might be implied that the DBD plasma generates active species, such as oxygen radicals, ozone, nitrogen oxide, as well as neutral and metastable molecules. These active species abstract the secondary hydrogen atom from polymeric chain to form the alkyl radicals. The alkyl radicals will further react with reactive oxygen species to form alkoxyl radicals. Both alkyl and alkoxyl radicals lead to the formation of the oxygen-containing polar functional groups, relating to an increase in the C-O, C=O and O-C=O bond [7]. These results were in agreement with the FTIR results.

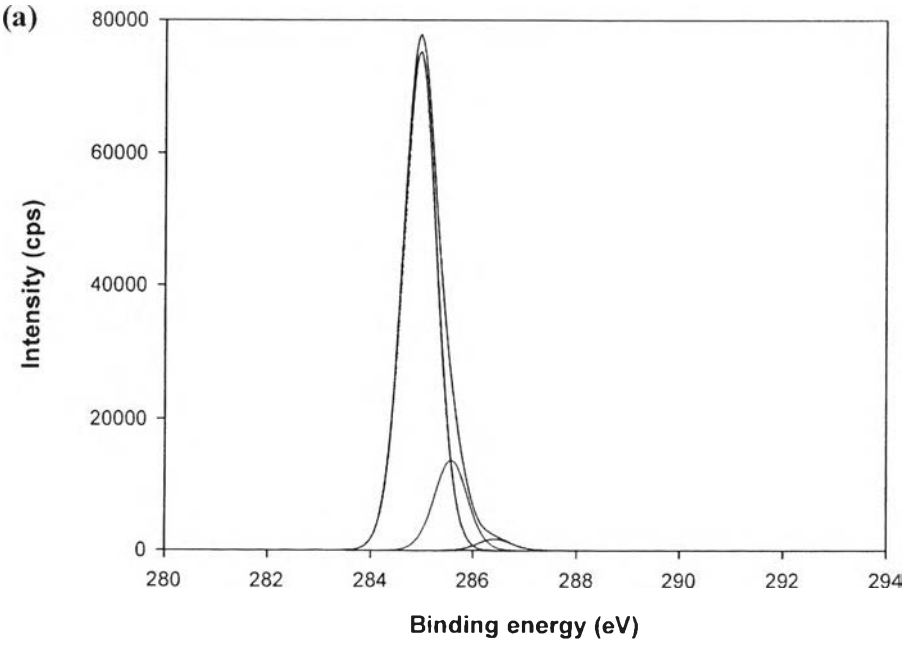

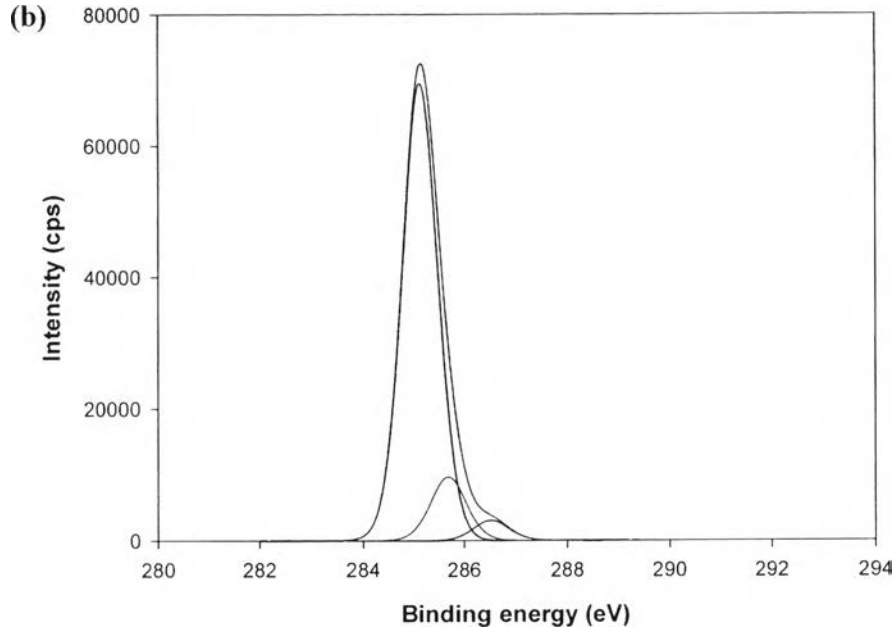

Figure 4.5 XPS spectra of (a) untreated-PP films and (b) plasma-treated PP films at 10 s.

Table 4.1 Effect of plasma treatment time on the percentage of chemical composition

Treatment time (s)	Percentage of chemical composition				
	285.0 eV C-C/C-H	285.8 eV C-CO_2	287.1 eV C-O	288.5 eV C=O	289.7 eV O-C=O
0	84.5	14.1	1.4	-	-
10	83.5	13.1	3.4	-	-
20	37.8	44.9	8.3	5.5	3.5
40	29.2	47.7	10.5	7.6	5.0
90	23.3	50.3	11.7	7.7	6.9

4.4.1.4 Effect of DBD Plasma Treatment Time on Surface Morphology of PP Film.

Changes in the surface topography of the PP films after the DBD plasma treatment were examined by using the SPM technique. Figure 4.6 show three-dimentional SPM images of the PP sample both before and after the DBD plasma treatment at different treatment times. Root mean square roughness (R_{rms}) was used to represent surface roughness of PP sample. The results revealed that the surface roughness of PP-films increased abruptly after plasma treatment time 10 s (R_{rms} = 28.90 nm ± 3.52 nm) which was 8 times greater than the value of the untreated one (R_{rms} = 3.67 nm ± 0.33). Beyond 10 s, the roughness of PP films further increased to 29.2153 nm ± 2.13 nm, 38.33 nm ± 5.90 nm, and 59.27 nm ± 5.67 nm as the plasma treatment time increased to 20 s, 30 s, and 40 s, respectively. The surface morphology changed due to the reactive species generated by the plasma bombard the surface of PP film. Therefore, the chain scission occurred at the surface resulting in etching effect [4].

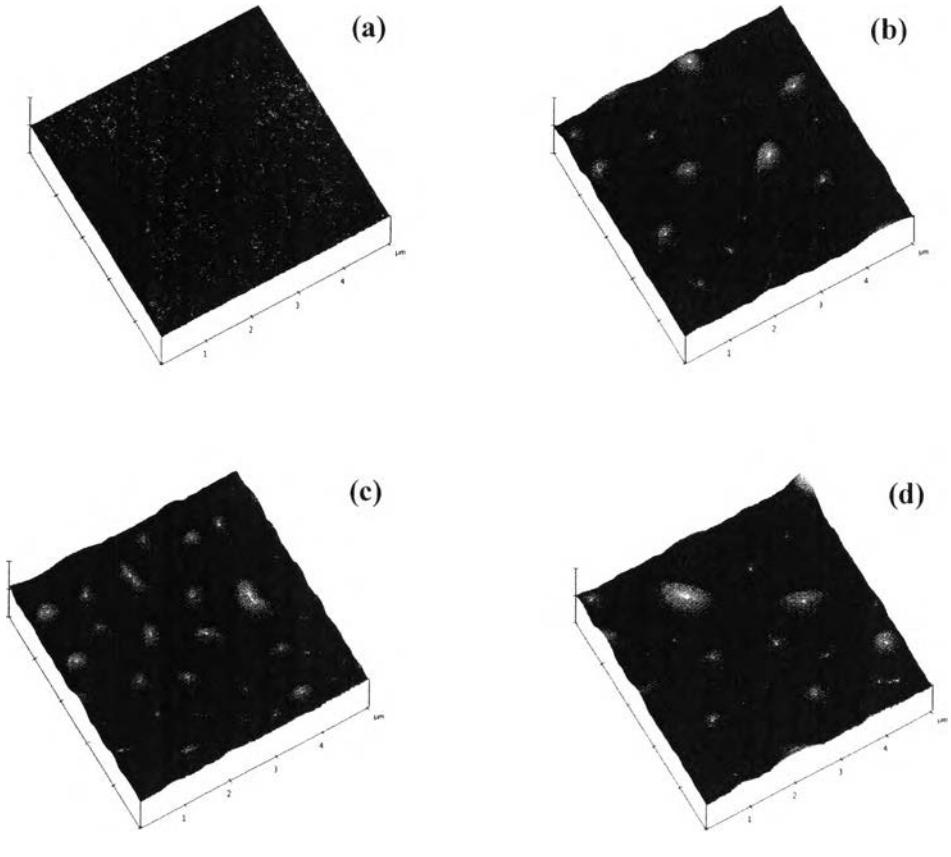

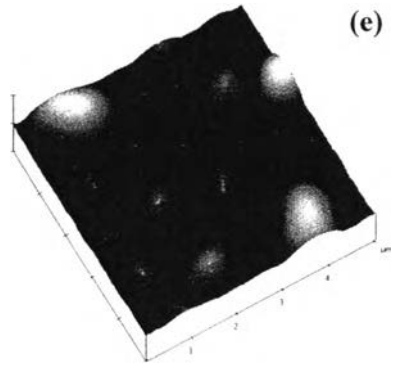

Figure 4.6 Three-dimentional SPA images of the PP sample: (a) untreated film, and DBD plasma-treated films at (b) 10 s, (c) 20s, (d) 30 s, and (e) 40 s.

4.4.2 Characterization of ZnO Nanoparticles

4.4.2.1 Crystallinity of ZnO Nanoparticles

The crystallographic of ZnO nanoparticles was examined by using the WAXD technique. As shown in Figure 4.7, the WAXD pattern of ZnO particles shows the presence of attributive peaks located at 2θ equal to 31.71°, 34.48°, 36.23°, 47.53°, 56.47°, 62.78°, and 67.92° which are associated with the (100), (002), (101), (102), (110), (103) and (112) planes, respectively [10]. It was indicated that the synthesized ZnO particles possessed hexagonal wurtzite crystal structure. It should be noted that the grain size of the test sample calculated by using the Scherrer formula based on the (101) diffraction peak is found to be 40.25 nm.

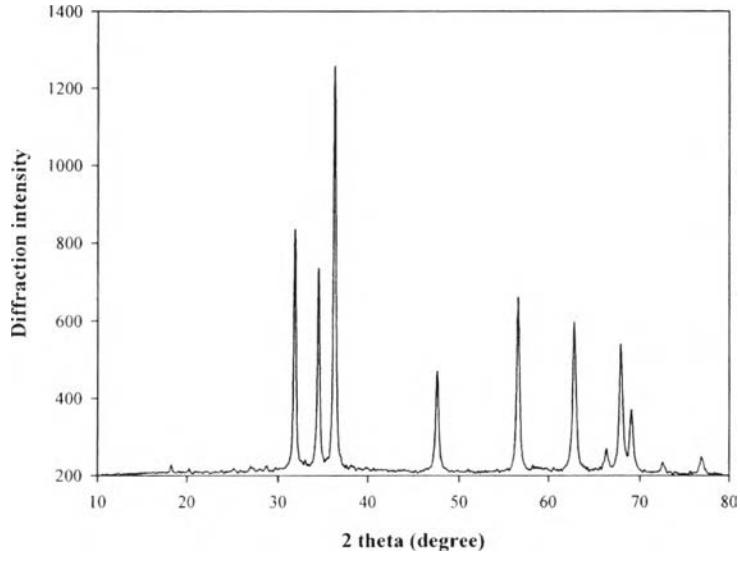

Figure 4.7 XRD pattern of ZnO nanoparticles.

4.4.2.2 Morphology of ZnO Nanoparticles

The morphology and the particle sizes of ZnO were examined by using the SEM. As shown in Figure 4.8, the synthesized ZnO particles are spherical with an average diameter of about 119 nm.

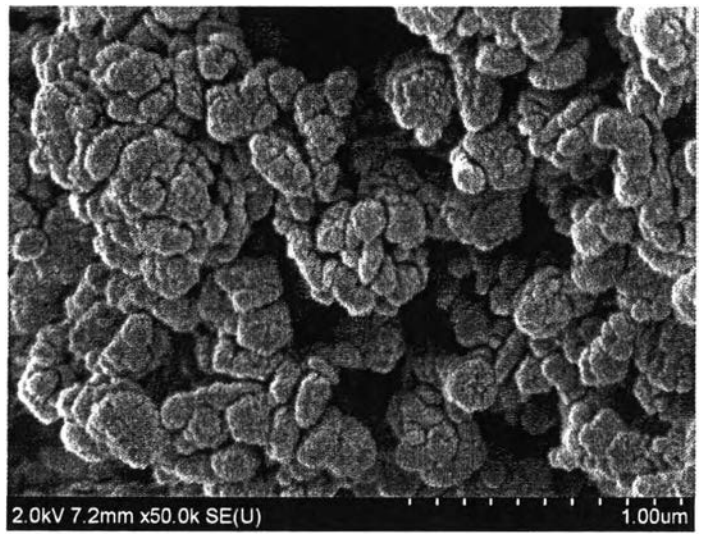

Figure 4.8 SEM images of the as-prepared ZnO nanoparticles.

4.4.3 ZnO Deposition on Plasma-Treated PP Film

4.4.3.1 Effect of DBD Plasma Treatment Time on ZnO Deposition

The amount of ZnO deposited on PP film was quantitatively determined by the AAS technique. Figure 4.9 shows the effect of DBD plasma treatment time on the amount of ZnO deposited on PP film. At any studied DBD plasma treatment time, the amount of ZnO deposited on the PP film remained constant at about 0.2 wt.%, indicating that the treatment time insignificantly affect the deposition of ZnO on the PP film. Therefore, the optimum time for the DBD plasma treatment of PP films was selected at 10 s.

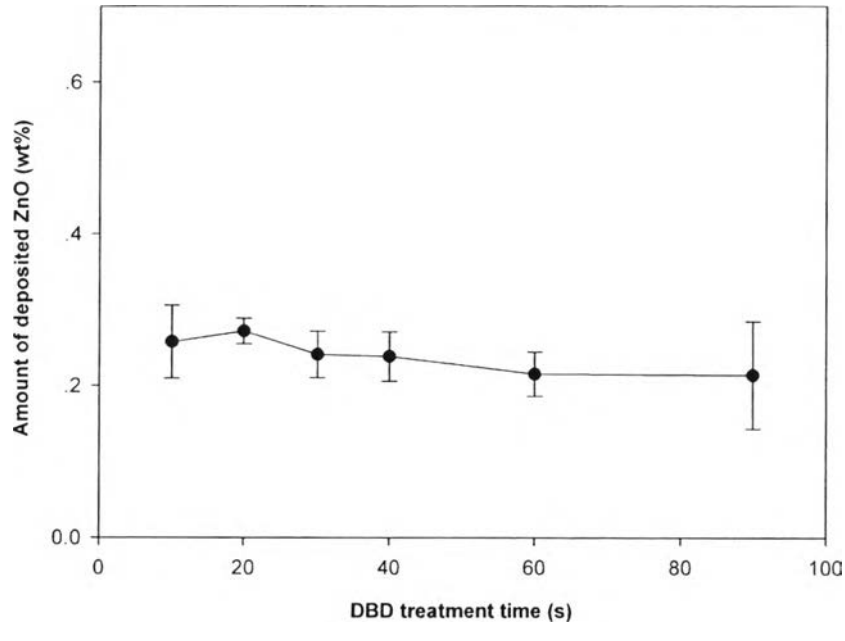

Figure 4.9 Effect of DBD plasma treatment time on amount of deposited ZnO.

4.4.3.2 The Distribution of ZnO Deposition on PP Films

The distribution of ZnO deposition on PP film was also observed with the use of the SEM-EDX technique. From Figures 4.10 and 4.11, the SEM micrographs clearly show a homogeneous distribution of ZnO particles on the PP surface.

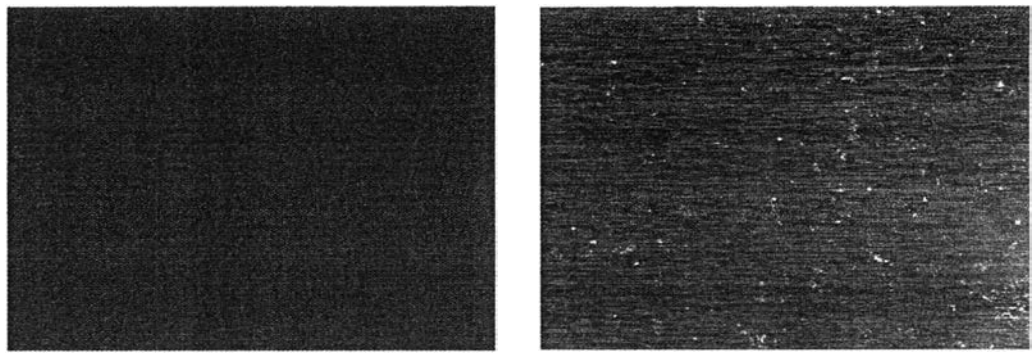

(a) (b)

Figure 4.10 SEM micrograph of (a) neat PP film and (b) ZnO-coated DBD plasma-treated PP film.

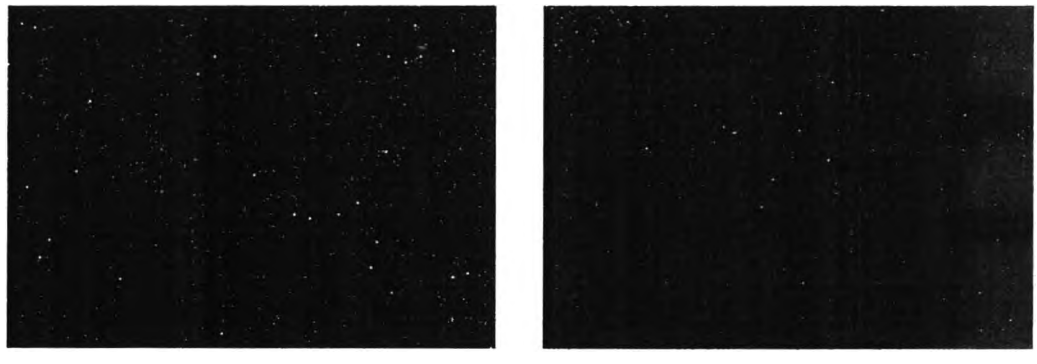

(a) (b)

Figure 4.11 SEM-EDX images of (a) Zn atom and (b) O atom distributed on ZnO-coated DBD plasma-treated PP surface.

4.4.3.3 Effect of Number Washing Cycle on Amount of ZnO Deposited on PP Films

To further verify whether or not the coating capability of the PP surface was enhanced after the plasma treatment, the amount of ZnO deposited on PP films was quantified with the use of the AAS. Figure 4.12 (a) shows the effect of number of washing cycles on the amount of ZnO deposited on PP films. It was found that the amount of ZnO deposited on surface decreased with increasing the number of washing cycles. After the ZnO-coated PP films were washed for two times, the amount of deposited ZnO on PP-fims became constant, suggesting the removal of

loosely bound ZnO on the PP surface. Therefore, two washing cycles was chosen for determination of the ZnO content.

Moreover, Figure 4.12 (b) show the amount of ZnO deposited on plasma-treated PP films compare to untreated PP films as a function of number washing cycles. It can be observed that the saturated amount of ZnO deposited on plasma-treated PP films was obtained after the samples were rinsed for two times. On the other hand, in case of untreated-PP films, the amount of ZnO deposited on the surfaces was gradually decreased and completely washed out as number of washing cycles increased. Consequently, the surface coating capability of PP films was improved by DBD plasma treatment.

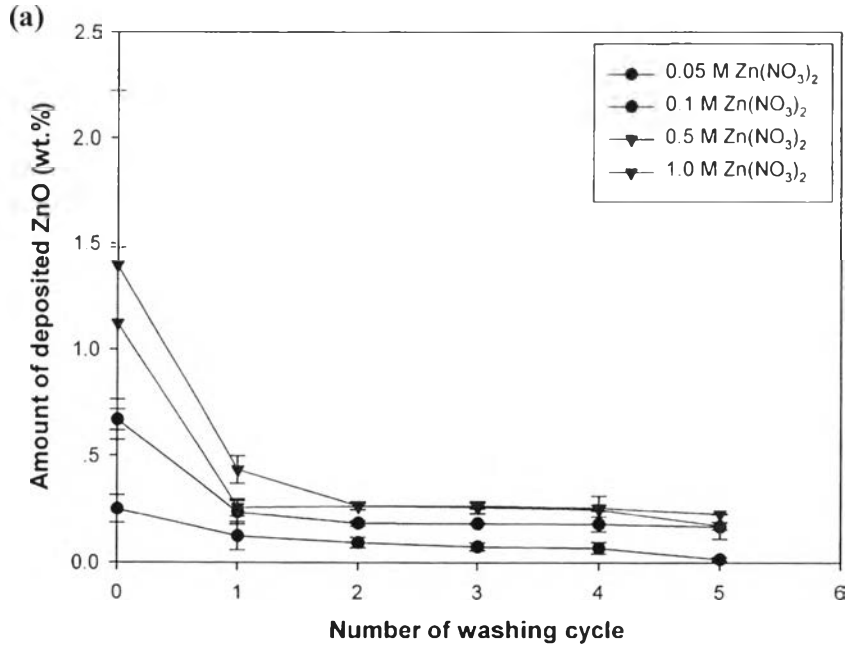

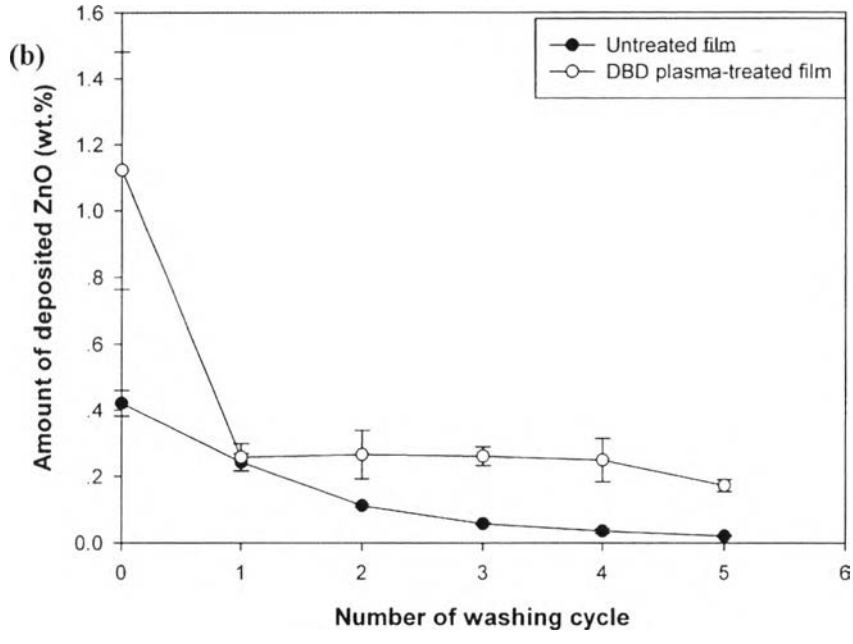

Figure 4.12 Effect of number of washing cycles on amount of ZnO deposited on PP films.

4.4.3.4 Effect of $Zn(NO_3)_2$ Concentration on Amount of ZnO Deposited on PP Films

The effect of $Zn(NO_3)_2$ concentration on the amount of ZnO deposited on PP films was studied at the optimum washing cycles. As shown in Figure 4.13, the amount of deposited ZnO increased with increasing the $Zn(NO_3)_2$ concentration from 0.05 M to 0.5 M before remaining constant at a $Zn(NO_3)_2$ concentration greater than 0.5 M. The result revealed that the highest amount of ZnO depostied on PP film was about 0.26 wt.%.

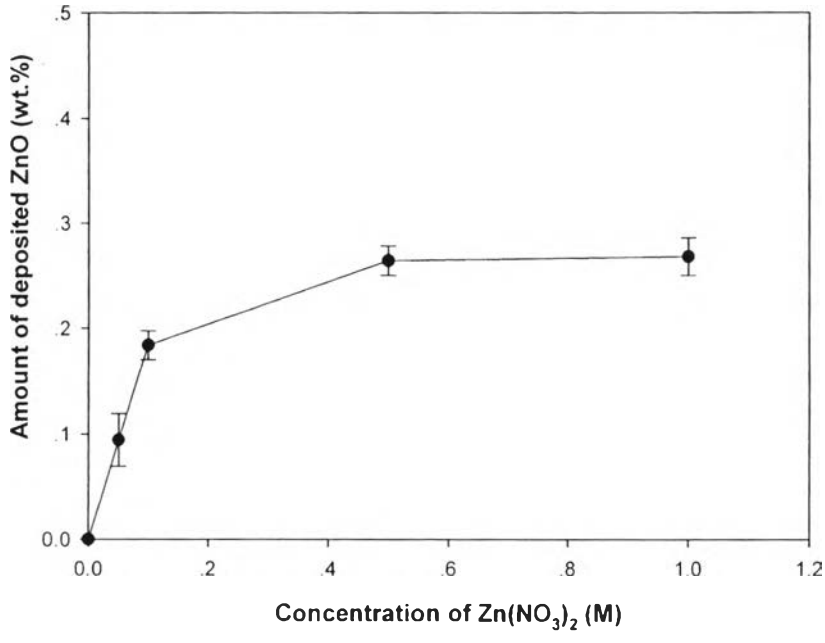

Figure 4.13 Effect of $Zn(NO_3)_2$ concentration on amount of deposited ZnO on PP-films.

4.4.3.5 ZnO Deposition on DBD Plasma-Treated PP Films

The chemical bonding between the plasma treated- PP films and the deposited ZnO nanoparticles was verified by the XPS technique. Figure 4.14 shows O 1s XPS spectra of ZnO-coated DBD plasma-treated PP films. The result indicated that the chemical composition of ZnO-coated DBD plasma-treated PP films showed three main peaks. The first peak located at 530.6 eV is corresponded to ZnO. The second peak located at 531.8 eV is corresponded to $Zn(OH)_2$ and the last peak located at 533.0 eV is corresponded to specific species, such as $-CO_3$, and adsorbed H_2O or adsorbed O_2 [6], [1]. It might be implied that the DBD plasma enhanced the coating ability of ZnO on PP surfaces via the deposition of ZnO as $Zn(OH)_2$. The percentages of ZnO, $Zn(OH)_2$, and other specific species are 72.0 %, 26.3 % and 1.7 %, respectively.

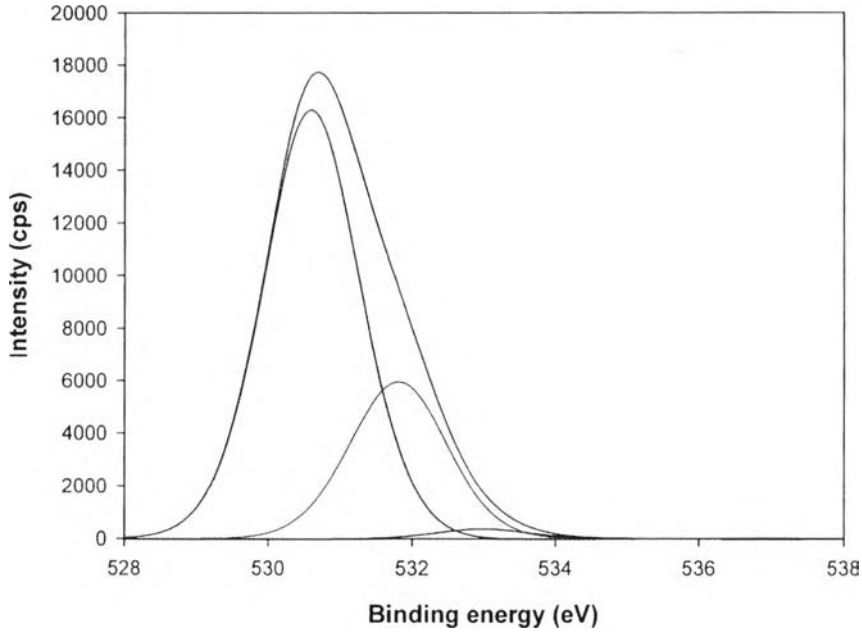

Figure 4.14 O 1s XPS spectra of ZnO-coated DBD plasma-treated PP films.

4.4.3.6 Effect of ZnO Coating on The Mechanical Properties of PP Films

The tensile strength and elongation at break of the PP films were also determined after the ZnO coating. As shown in Figures 4.15 (a) and (b), the deposited ZnO on plasma-treated PP films did not affect the mechanical properties of PP-films although an increase in the $Zn(NO_3)_2$ concentration increased the amount of ZnO deposited on the PP films. This is possibly because the ZnO nanoparticles was coated merely on the surface of treated-PP films. Hence, the ZnO nanoparticles did not interrupted the movement of PP chains [9].

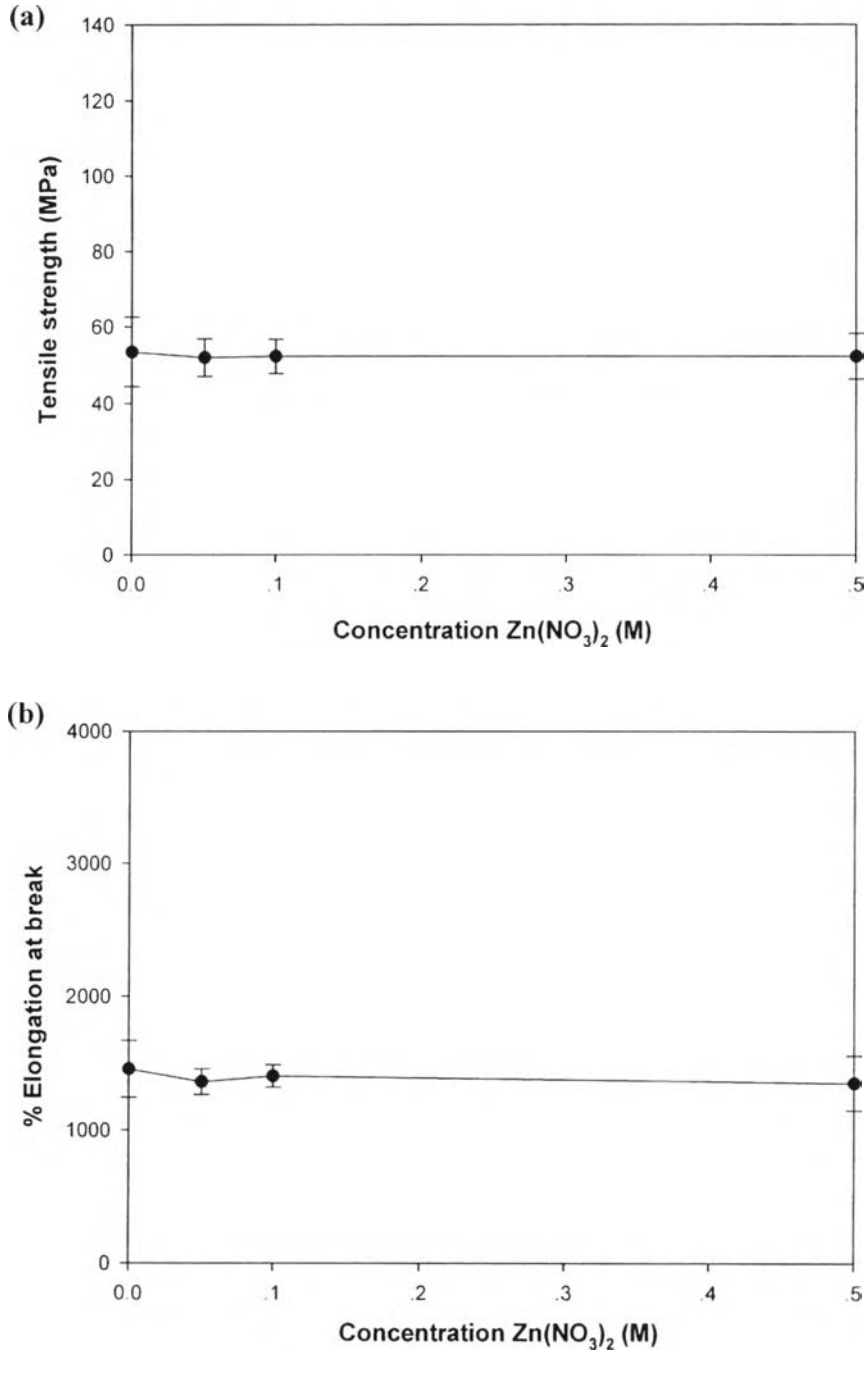

Figure 4.15 Effect of ZnO-coated PP films on (a) tensile strength and (b) elongation at break of PP-films.

4.4.4 Antibacterial Activities of ZnO-Coated DBD Plasma-Treated PP Films

To achieve the aim of this study, the antibacterial activity of neat PP and ZnO-coated PP films were determined. Table 4.2 (a) and (b) shows the percentage of bacterial reduction as a function of $Zn(NO_3)_2$ concentrations. The result indicated that an increase in the $Zn(NO_3)_2$ concentration increased the antibacterial activities of the ZnO-coated PP films. Furthermore, after the samples were illuminated with UV light for 3 h, the highest antibacterial activities against both *E.coli* and *S.aureus* were obtained. This can be possibly explained in that after ZnO-deposited PP films were illuminated with UV light, the reactive oxygen species (ROS) were generated. These ROS, such as H_2O_2 and OH•, are harmful to the living organism cells [8]. Compared between the two bacteria, the ZnO-coated PP films showed a lower percent of bacteria reduction against *S.aureus*. The result might be due to the fact that *S. aureus* has produced the oxidative stress-responsive genes which convert the reactive oxygen species to H_2O and O_2 which are not harmful to the cells [14]. However, the mechanism of ZnO to perform the antibacterial activities has still under investigated.

Table 4.2 (a) Colony forming unit (cfu) counts at 0 and 3 h incubation time intervals of ZnO-coated PP films against *E.coli* with UV light

Incubation time	***E.coli (cfu/ml)***				
	Blank w/o PP	**Original PP**	**$Zn(NO_3)_2$ concentration (M)**		
			0.05	**0.1**	**0.5**
0 h	9.1×10^6	9.1×10^6	9.1×10^6	9.1×10^6	9.1×10^6
3 h	3.3×10^6	3.2×10^6	1.8×10^5	1.0×10^5	0.2×10^5
% decrease /increase	decrease 63.7%	decrease 63.7%	decrease 98.0%	decrease 98.9%	decrease 99.8%

Table 4.2 (b) Colony forming unit (cfu) counts at 0 and 3 h incubation time intervals of ZnO-coated PP films against *S.aureus* with UV light

Incubation time	***S.aureus (cfu/ml)***				
	Blank w/o PP	**Neat PP**	**$Zn(NO_3)_2$ concentration (M)**		
			0.05	**0.1**	**0.5**
0 h	2.3×10^6	2.3×10^6	2.3×10^6	2.3×10^6	2.3×10^6
3 h	1.8×10^6	1.8×10^6	4.6×10^5	2.3×10^5	0.8×10^5
% decrease /increase	decrease 21.7%	decrease 21.7%	decrease 80.0%	decrease 90.0%	decrease 96.5%

Moreover, the neat PP and ZnO-coated PP films were also tested without UV light and the contact interval time was 24 h. Table 4.3 (a) and (b) show the antibacterial activities of neat PP and ZnO-coated PP films against *E.coli* and *S.aureus*, respectively. It was observed that the highest antibacterial activities of ZnO- coated PP films were obtained although the samples were not exposed to the UV light. These results might be explained that the ZnO nanoparticles on treated- PP film contacted to the cell membrane of bacteria resulting in occurring cell membrane rupture and minerals, proteins and genetic materials were leaked out, causing cell death [13].

As mentioned above, the ZnO- coated PP films could performed the antibacterial activities with and without UV light. Therefore, it should be possibly used as the antibacterial packaging in order to keep the quality of food products.

Table 4.3 (a) Colony forming unit (cfu) counts at 0 and 24 h incubation time intervals of ZnO-coated PP films against *E.coli* without UV light

Incubation time	*E.coli (cfu/ml)*				
	Blank w/o PP	Original PP	$Zn(NO_3)_2$ concentration (M)		
			0.05	0.1	0.5
0 h	1.2×10^{7}	1.2×10^{7}	1.2×10^{7}	1.2×10^{7}	1.2×10^{7}
24 h	7.1×10^{7}	8.3×10^{7}	1.0×10^{6}	1.0×10^{5}	3.3×10^{4}
% decrease /increase	increase 491%	increase 591%	decrease 91.7%	decrease 99.2%	decrease 99.8%

Table 4.3 (b) Colony forming unit (cfu) counts at 0 and 24 h incubation time intervals of ZnO-coated PP films against *S.aureus* without UV light

Incubation time	*S.aureus (cfu/ml)*				
	Blank w/o PP	Original PP	$Zn(NO_3)_2$ concentration (M)		
			0.05	0.1	0.5
0 h	1.0×10^{6}	1.0×10^{6}	1.0×10^{6}	1.0×10^{6}	1.0×10^{6}
24 h	4.3×10^{5}	7.5×10^{5}	1.0×10^{4}	6.6×10^{3}	3.3×10^{3}
% decrease /increase	decrease 57.0%	decrease 25.0%	decrease 99.0%	decrease 99.3%	decrease 99.6%

4.5 Conclusions

In this works, the surface modification of PP-film was operated via DBD plasma in air. The results show that the hydrophilicity of treated-PP film was increased due to the incorporation of oxygen-containing polar groups, including C-O, C=O and O-C=O. However, the mechanical properties of treated-PP film was not changed because PP film was modified only the uppermost of surfaces. Therefore, the DBD plasma technique was a suitable process to enhance the coating capability of the film surfaces, whereas the bulk properties were remain. After that the plasma-

treated PP film was further immersed in zinc nitrate solution before being converted to zinc oxide particles by reacting with NaOH. The saturated amount of ZnO deposited on treated-PP film was determined. It was found that the ZnO deposited on treated-PP film performed strong antibacterial against both *E.coli* (Gram negative) and *S.aureus* (Gram positive) when it was illuminated with UV light for 3 h. As a result, the ZnO deposited treated-PP film can be used as the antibacterial packaging in order to keep the quality of food products.

4.6 Acknoeledgements

The first author is grateful for the scholarship and funding to this study provided by the Petroleum and Petrochemical College and by the Center of Excellence on Petrochemical and Materials Technology, Thailand.

4.7 References

[1] Chen, M., Wang, X., Yu,Y.H., Pei, Z.L., Bai, X.D., Sun, C., Huang, R.F., and Wen, L.S. (2000). X-ray photoelectron spectroscopy and auger electron spectroscopy studies of Al-doped ZnO films. Applied Surface Science, 158(1-2), 134-140.

[2] Chiang, M.H., Liao, K.H., Lin, I.M., Lu, C.C., Huang, H.Y., Kuo, C.L., and Wu, J.S. (2010). Modification of hydro property of polypropylene films by a parallel-plate nitrogen-based dielectric barrier discharge jet. IEEE Transactions on Plasma Science, 38(6), 1489-1497.

[3] Cui, N.Y., and Brown, N.M.D. (2002). Modification of the surface properties of a polypropylene film using and air dielectric barrier discharge plasma. Applied Surface Science, 189(1-2), 31-38.

[4] Esena, P., Riccardi, C., Zanini, S., Tontini, M., Poletti, G., and Orsini, F. (2005). Surface modification of PET film by a DBD device at atmospheric pressure. Surface and Coatings Technology, 200(1-4), 664-667.

[5] Esena, P., Zanini, S., and Riccardi, C. (2008). Plasma processing for surface optical modifications of PET films. Vacuum, 82(2), 232-235.

[6] Eisele, W., Ennaoui, A., Bischoff, P.S., Giersig, M., Pettenkofer, C., Krauser, J., Stiener, M.L., Zweigart, S., and Karg, F. (2003) XPS, TEM and NRA investigations of $Zn(Se,OH)/Zn(OH)_2$ films on $Cu(In,Ga)(S,Se)_2$ substrates for highly efficient solar cells. Solar Energy Material and Solar Cells, 75(1), 17-26.

[7] Geyter, N.D., Morent, R., Leys, C., Gengembre, L., and Payen, E. (2007). Treatment of polymer films with a dielectric barrier discharge in air, helium and argon at medium pressure. Surface and Coatings Technology, 201(16-17), 7066-7075.

[8] Ghule, K., Vithal, A., Chen, B., and Ling, Y., (2006). Preparation and characterization of ZnO nanoparticles coated paper and its antibacterial activity study . Green Chemistry, 8(12) , 1034-1041.

[9] Li, D., and Haneda, H. (2003). Morphologies of zinc oxide particles and their effects on photocatalysis. Chemosphere, 51(2), 129-137.

[10] Moafi, H.F., Shojaie, A.F., and Zanjanchi, M.A. (2011). Photocatalytic self-cleaning properties of cellulosic fibers modified by nano-sized zinc oxide. Thin Solid Films, 519(11), 3641-3546.

[11] Morent, R., Geyter, N.D., Leys, C., Gengembre, L., and Payen, E. (2007). Comparison between XPS- and FTIR-analysis of plasma-treated polypropylene film surfaces. Surface and Interface Analysis, 40(3-4), 597-600.

[12] Onsuratoom, S., Rujiravanit, R., Sreethawong, T., Tokura, S., and Chavadej, S. (2009), Silver loading on DBD plasma-modified woven PET surface for antimicrobial property improvement. Plasma Chem Plasma Process, 30(1), 191-206.

[13] Padmavathy, N., and Vijayaraghavan, R. (2008). Enhanced bioactivity of ZnO nanoparticles-an antibacterial study. Science and Technology of Advanced Material, 9(3), 1-7.

[14] Quintavalla, S., and Vicini, L. (2002). Antimicrobial food packaging in meat industry. MEAT SCIENCE, 62(3), 373-380.

[15] Raghupathi, K.R., Koodali, R.T., and Manna, A.C. (2011). Size-dependent bacterial growth inhibition and mechanism of antibacterial activity of zinc oxide nanoparticles. Langmuir, 27(7), 4020-4028.

[16] Ragojanu. A., Rusu, E., and Dorohoi, D.O. (2010). Characterization of structural modifications induced on poly(vinyl alcohol) surface by atmospheric pressure plasma. International Journal of Polymer Analysis and Characterization, 15(4), 210-221.

[17] Ruffolo, S.A., Russa, M.F.La., Malagodi, M., Rossi, C.O., Palermo, A.M., and Crisci, G.M. (2010). ZnO and $ZnTiO_3$ nanopowders for antimicrobial stone coating. Applied Physics A Material Science and Processing, 100(3), 829-834.

[18] Tayel, A.A., Tras, W.F., Moussa, S., Baz, A.F., Mahrous, H., Salem, M.F., and Brimer, L. (2011). Antibacterial action of zinc oxide nanoparticles against foodborne pathogens. Journal of Food Safety, 31(2), 211-218.

[19] Tendero, C., Tixier, C., Tristant, P., Desmaison, J., and Leprince, P. (2006). Atmospheric pressure plasma : A review. Spectrochimica Acta Part B, 61(1), 2-30.

[20] Watthanaphanit, A., Supaphol, P., Tamura, H., Tokura, S. and Rujiravanit, R. (2010) Wet-spun alginate/chitosan whiskers nanocomposite fibers: Preparation, characterization and release characteristic of the whiskers. Carbohydrate Polymers, 79, 738-746.